



## Cadmium Ions Pollution Treatments in Aqueous Solution Using Electrochemically Synthesized Gamma Aluminum Oxide Nanoparticles with DFT study



Dhia H. Hussain<sup>(1)</sup>, Ahmed M. Rheima<sup>\*(2)</sup>, Shaimaa H. Jaber<sup>(1)</sup>, Mustafa M. kadhim<sup>(2)</sup>

<sup>(1)</sup>Department of Chemistry, College of Science, University of Mustansiriyah, Baghdad, Iraq.

<sup>(2)</sup>Department of Chemistry, College of Science, Wasit University, Wasit, Iraq

$\gamma$ -Al<sub>2</sub>O<sub>3</sub> nanoparticles have been synthesized by electrochemical method using a rectangular aluminum plate as the anode and aluminum plate as the cathode (counter electrode); both electrodes have the same shape and dimensions. TEM, and XRD have been used to characterize the nanoparticles. The results indicated that the size range of  $\gamma$ -Al<sub>2</sub>O<sub>3</sub> nanoparticles was (14- 19) nanometers. Dealt with the studying of the effectiveness of the synthesized nanoparticles on the adsorption of cadmium ion from its aqueous solutions under different temperatures (10, 20, 30, 40, 50) °C. Also thermodynamic parameters ( $\Delta S$ ,  $\Delta H$ ,  $\Delta G$ ) were calculated. The equilibrium geometries of  $\gamma$ -Al<sub>2</sub>O<sub>3</sub> nanoparticles have been studied by Density function theory (DFT) using Gaussian 09 package program. The calculated highest-occupied molecular orbital energy ( $E_{\text{HOMO}}$ ) is to be (-0.04798 a.u) and the lowest-unoccupied molecular orbital energy ( $E_{\text{LUMO}}$ ) is to be (0.05909 a.u). The calculated activation energy breakage  $\gamma$ -Al<sub>2</sub>O<sub>3</sub>-Cd was (35.529 kcal/mole).

**Keywords:**  $\gamma$ -Al<sub>2</sub>O<sub>3</sub> Nanoparticles, Electrochemical, Cadmium ion, Pollution, TEM, XRD, DFT.

### 1- INTRODUCTION

The abundant compound of aluminum and oxygen is aluminum oxide with chemical formula Al<sub>2</sub>O<sub>3</sub>. It is the most prevalent event of many aluminum oxides, identified as aluminum oxide (III) in specific. It is frequently referred to as alumina. Due to their hardness, elevated melting point, chemical inertia, non-volatility and resistance to oxidation and corrosion, aluminum oxides are commonly used in refractories, ceramics and abrasives [1-3]. Al<sub>2</sub>O<sub>3</sub> nanopowder

has a wide variety of programs including digital ceramics, excessive amounts of electricity and catalysts. Also commonly acknowledged was the significance of alumina as a catalyst or catalyst for many chemical reactions[4]. The transparency of thin films in alumina and their broad use in home accessories have helped to boost their optical applications [5]. Al<sub>2</sub>O<sub>3</sub> nanopowder is an outstanding thermal conductor, but an electrical insulator. Aluminum oxide or  $\alpha$  Aluminum oxide nanopowder is usually the highest crystalline type of aluminum oxide and its hardness makes it

\*Corresponding author e-mail: [arahema@uowasit.edu.iq](mailto:arahema@uowasit.edu.iq)

Received 11/9/2018; Accepted 11/11/2019

DOI: 10.21608/ejchem.2019.16882.2026

©2020 National Information and Documentation Center (NIDOC)

appropriate as an abrasive layer of fabric and has become a significant factor in cutting equipment [6]. Quantum chemical techniques have already proved very helpful in the determination of the molecular structure and in the elucidation of the electronic structure and reactivity [7, 20]. Thus, computational chemistry calculations in research of corrosion inhibition, biological activity and nonlinear optical (NLO) characteristics have become a prevalent practice [8].

## 2- EXPERIMENTAL

### 2.1 CHEMICALS AND REAGENTS

All the chemicals were of analytical reagent grades and used as received, without further purifications.

### 2.2 SYNTHESIS OF $\gamma$ -Al<sub>2</sub>O<sub>3</sub> NANOPARTICLES

$\gamma$ -Al<sub>2</sub>O<sub>3</sub> nanoparticles have been synthesized by electrolysis using 125 ml of 0.05 M NaOH at 25 °C as electrolyte. A rectangular aluminum plate (40 mm x 20 mm x 1 mm) was used as anode and same dimensions rectangular aluminum plate was used as the counter electrode

$$Q_e = \frac{(C_o - C_e)V_{sol}}{M} \quad (1)$$

Where  $Q_e$  is the capacity at equilibrium (mg/g),  $C_o$  is the initial concentration of the ion in the solution (mg/l),  $C_e$  is the ion concentration at equilibrium (mg/l),  $V$  is the solution volume (l) and  $M$  is the adsorbent mass (g).

## 3- RESULTS AND DISCUSSION

The synthesized  $\gamma$ -Al<sub>2</sub>O<sub>3</sub> nanoparticles by electrochemical method had been characterized by X-Ray Diffractometry Analysis (XRD) and Transmitted Electron microscope (TEM).

(cathode). Before mounting the substrates in the cell, they are cleaned sonically using aqueous and organic solvents as a cleaner (ethanol, acetone, chloroform, de-ionized water) sequentially, each cleaning step duration was 3 minutes. The applied D.C. voltage between the electrodes was 3 V under current density of  $4.19 \times 10^{-3}$  mA/cm<sup>2</sup> for 5 h. A brown precipitate was obtained, the product washed with de-ionized water then dried overnight. Then characterized by XRD and TEM.

### 2.3 ADSORPTION EXPERIMENTS

A stock solution of (150 mg/l) cadmium ion was prepared by dissolving Cd(NO<sub>3</sub>)<sub>2</sub> in de-ionized water. The solution had further dilution to the required concentrations (10 - 50 mg/l) of cadmium ion. All the experiments had been performed by agitating 100 ml of cadmium solution at the desired concentration and 0.05 g of  $\gamma$ -Al<sub>2</sub>O<sub>3</sub> nanoparticles in 10 ml glass tubes. The glass tubes were shaken for 100 min at (10, 20, 30, 40, 50) °C. Cadmium concentration was determined using atomic absorption spectrometer. The retained concentration of cadmium ion in the adsorbent phase determined according to

XRD patterns of the  $\gamma$ -Al<sub>2</sub>O<sub>3</sub> nanoparticles recorded in the  $2\theta$  range of 10 to 80° are shown in Fig. 1. The diffraction peaks in the samples observed around  $2\theta = 19^\circ, 31^\circ, 37^\circ, 45^\circ, 56^\circ, 60^\circ$  and  $66^\circ$  corresponding to the (111), (220), (311), (400) (422), (511) and (440) were due to the structure of the  $\gamma$ -Al<sub>2</sub>O<sub>3</sub> [JCPDS No. 29-0063].

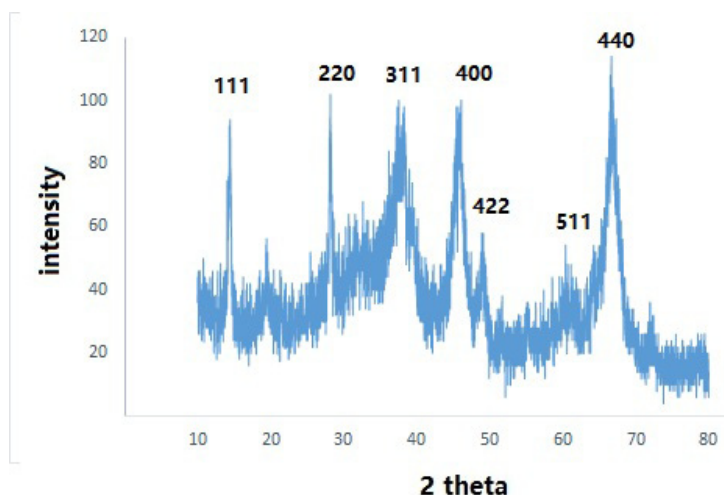


Figure 1. XRD pattern of  $\gamma$ - $\text{Al}_2\text{O}_3$  nanoparticles.

There are significant amounts of broad lines (peaks) which are characteristic to nanoparticles. Debye-Scherrer equation had been used to calculate the crystallite size of  $\gamma$ - $\text{Al}_2\text{O}_3$  nanoparticles [9].

$$D = (k \lambda) / (\beta \cos \theta) \quad (2)$$

Scherrer constant  $k = 0.9$ , the wavelength of the  $\text{Cu-K}\alpha$  radiations and the full width at half maximum symbolized by  $(\lambda)$  and  $(\beta)$  respectively,  $\theta$  is the angle calculated

from  $2\theta$  values which corresponding to the maximum intensity peak in XRD pattern. The mean crystallite size of nanoparticles which calculated by Debye-Scherrer equation was 14.3 nm. The use of Scherrer's equation to the (440) reflection peaks indicated the formation of  $\gamma$ - $\text{Al}_2\text{O}_3$  [JCPDS No. 29- 0063].

Fig. 2 shows TEM image of  $\gamma$ - $\text{Al}_2\text{O}_3$  nanoparticles. It is observed that the synthesized  $\gamma$ - $\text{Al}_2\text{O}_3$  nanoparticles have a typical average diameter less than 19 nm.

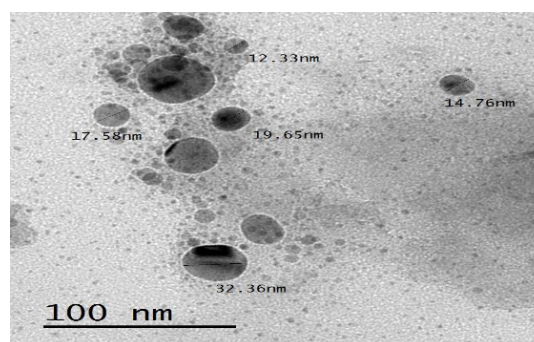
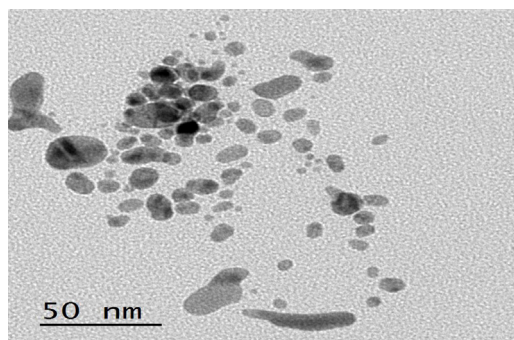


Figure 2. TEM image of  $\gamma$ - $\text{Al}_2\text{O}_3$  nanoparticles.

### 3.1 ADSORPTION ISOTHERM

The cadmium adsorption isotherm undergo to the linearized Freundlich isotherm, as shown in Fig. 3. The relation between the adsorption capacity  $Q_e$  (mg/g) of  $\gamma$ - $\text{Al}_2\text{O}_3$  nanoparticles and the  $\text{Cd}^{2+}$  concentration  $C_e$  (mg/L) at equilibrium is given by

$$\log(Q_e) = \log(k_f) + (1/n)\log(C_e) \quad (3)$$

The symbols  $K_f$  and  $n$  symbolizes the Freundlich constants which have indicated the capacity and the intensity of the adsorption respectively. The data of the isotherm well fitted the Freundlich isotherm ( $R^2=0.985$ ). The constants values ( $K_f$  and  $n$ ) had been calculated to be 14.09 and 0.324, respectively. The value of ( $n$ ) indicated multilayer adsorption.

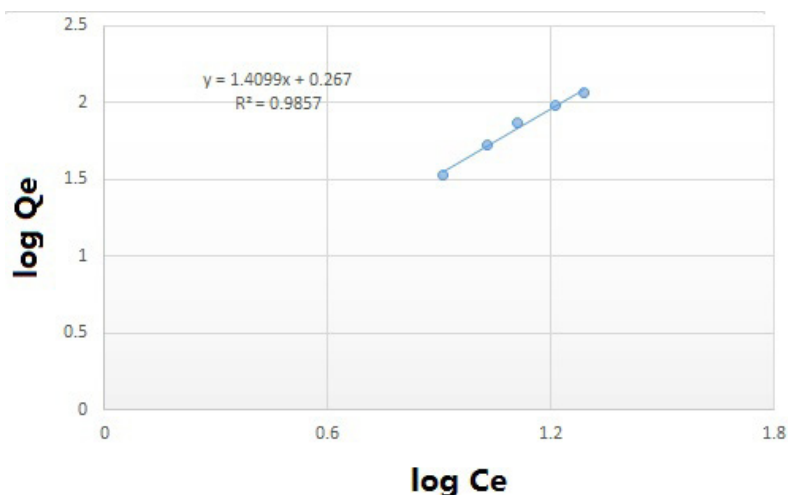


Figure 3. Adsorption equation of Freundlich isotherm, at 293 K

Equation (4) expresses the Langmuir isotherm:

$$\frac{C_e}{Q_e} = \frac{1}{a} + \frac{b}{a} C_e \quad (4)$$

Langmuir constants  $a$  and  $b$  are related to the energy of adsorption. Adsorption curves of cadmium in their solution fitted with Langmuir isotherm as shown in the relation between  $(C_e)$

versus  $(C_e / Q_e)$  in fig.4 and the results show that they do not undergo to the Langmuir isotherm, due to Langmuir isotherm limited mainly by two factors, Langmuir isotherm, which is applicable for monolayer surface sorption with a limited amount of homogeneous energy sites [10].

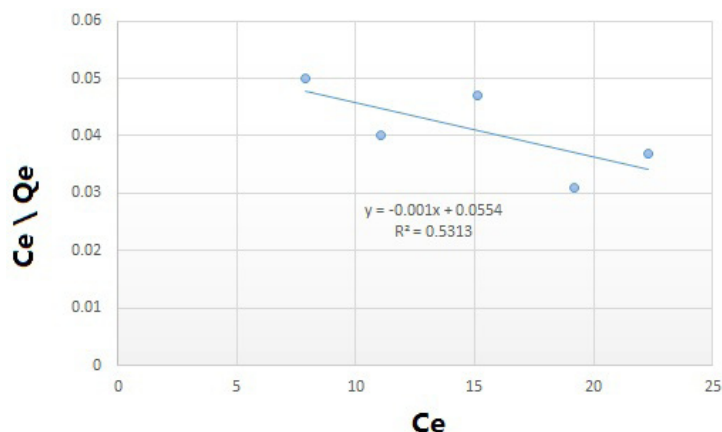


Figure 4. Adsorption equation of Langmuir isotherm, at 293 K

### 3.2 THERMODYNAMIC PARAMETERS

The adsorption of cadmium on  $\gamma$ -Al<sub>2</sub>O<sub>3</sub> nanoparticles had been studied as temperature dependent function. Experiments were done at different temperatures (10, 20, 30, 40 and 50°C). The results indicated that the adsorption increases

with increasing in temperature, this is primarily due to the enhanced surface activity, meaning the process is endothermic ( $\Delta H$  is positive).

The following equations were used to calculate the changes in gibs free energy of adsorption ( $\Delta G$ ), enthalpy ( $\Delta H$ ), and entropy ( $\Delta S$ ):

$$\log KC = \frac{-\Delta H}{2.303RT} + \frac{\Delta S}{R} \quad (5)$$

$$\Delta G = -RT \ln K_c \quad (6)$$

$$Kc = \frac{C_{Ac}}{C_e} \quad (7)$$

The symbols  $K_c$ ,  $C_e$ ,  $C_{Ac}$ ,  $R$  and  $T$  symbolize the equilibrium constant, is the equilibrium concentration in solution (mg/L), is the equilibrium concentration of solid-phase, the general constant of gases (8.314 J/mol K) and the temperature (K) respectively.  $\Delta H$  and ( $\Delta S$ ) had been calculated from the slope and intercept of the van't Hoff plots of  $\log(K_c)$  versus  $1/T$  [11], as shown in Fig. 5

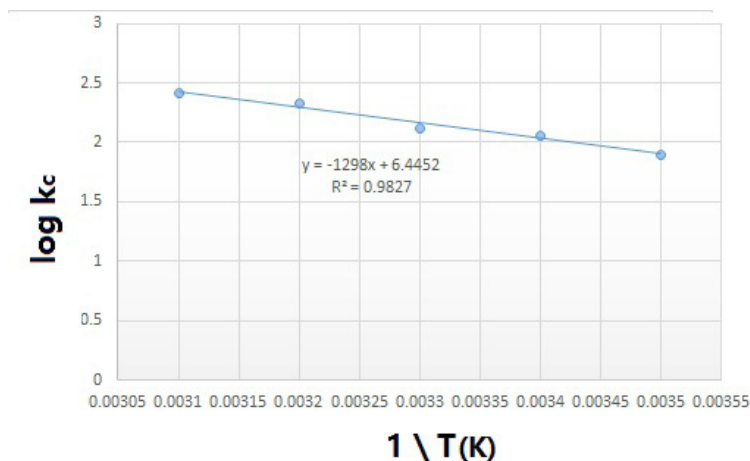


Figure 5. Relation between  $\log K_c$  and  $1/T$  for the adsorption of cadmium ions.

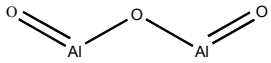
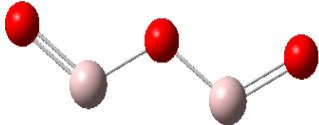
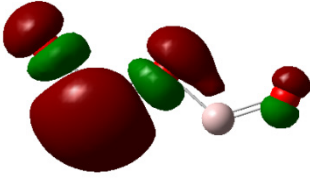
The calculated values of  $\Delta H$  and  $\Delta S$  in this work were 24.85 kJ/mol and 53.58 J/(mol·K) respectively, the positive value of  $\Delta H$  indicates that the adsorption process is endothermic and the adsorption capacity increases with increasing temperature, the positive value of  $\Delta S$  indicate increasing entropy which are attributable to the occurrence of the absorption as well as adsorption process, these results suggest that the higher temperature facilitated the adsorption of cadmium. The negative  $\Delta G$  value for the adsorption (-11.024 kJ/mol) at 293 K indicates that the adsorption happens spontaneously in nature.

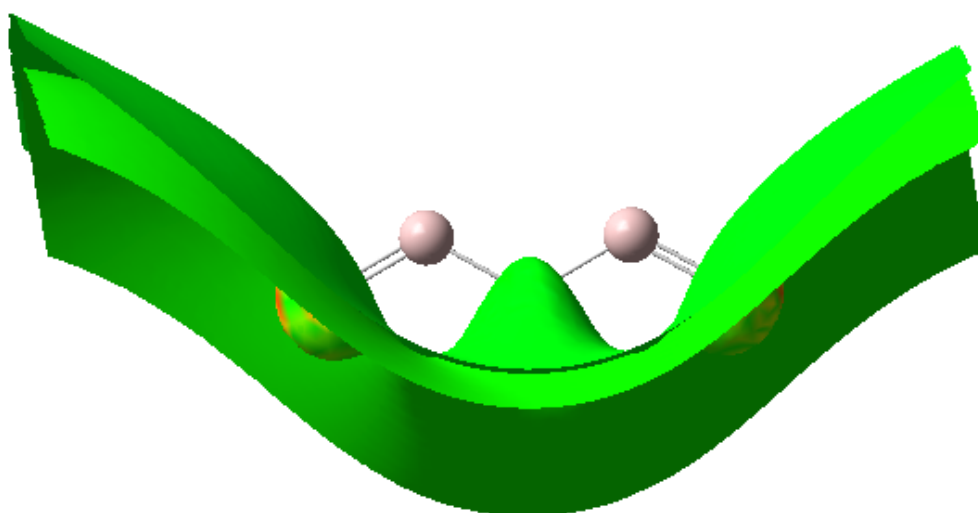
### 3-3 THEORETICAL STUDY

The construction of the compounds was built using Gaussian 09 package program [12] then equilibrium geometries were calculated by DFT method. Unrestricted Density Functional Theory

(U-DFT/STO-3G) level [13,14] for calculating the geometry of the investigated molecule in vacuum medium. The final geometry and HOMO-LUMO orbitals of a compound based on the most correct method DFT are given in **Table 1**. The highest-occupied molecular orbital energy ( $E_{HOMO}$ ) equal to (-0.04798 a.u), the lowest-unoccupied molecular orbital energy ( $E_{LUMO}$ ) is (0.05909 a.u). The point group of the molecule ( $C_2V$ ). Electrostatic surface potential represents the direct adsorption of molecule surface cadmium ion **Fig. 7** according to more nucleophilic sites [15]. This result corresponds to what has been obtained in experimental part of this work, since the negative value of the calculated  $\Delta G$  refers to the automatic adsorption process in normal conditions.

Table 1: Compound in two, three dimension and molecule orbitals.

Comps.	2D	3D	HOMO-LUMO MO
Al <sub>2</sub> O <sub>3</sub>			

Figure 6: Electrostatic surface potential for Al<sub>2</sub>O<sub>3</sub>

### 3-4 CALCULATIONS OF O-Cd BOND BREAKAGE ENERGY

The energy of breakage activation AL<sub>2</sub>O<sub>3</sub>-Cd was calculated using method of reaction coordinate [16]. Just the length of the OA bond is restricted to the appropriate degree of freedom while all other bond lengths were freely optimized. In the DFT procedure (Ea<sup>#</sup>= E transition state- E reactant) the values of activation energy for the OCd fracture, reactions were calculated from the differences between the energies of the worldwide optimize models and the derived transition states. The activation energies

acquired from the level of Unrestricted Functional Density Theory (U-DFT / STO-3 G) were calculated without any solvent being included. It has been shown in previous research that the U-DFT / STO-3 G produces a sudden decrease in complete molecular energy after the transition state (t.s) for the OCd bond rupture reaction path. [17-19] **Fig. 8** shows the calculated reaction sequence for AL<sub>2</sub>O<sub>3</sub>-Cd cracking mechanisms. The significant negative ΔEc value (exothermic reaction) of DFT (ΔEc= -15.499 kcal/mol) with activation energy Ea<sup>#</sup>value by DFT (35.529 kcal/mol). As a consequence the ions from the AL<sub>2</sub>O<sub>3</sub> molecules are easily removed after adsorption [20].

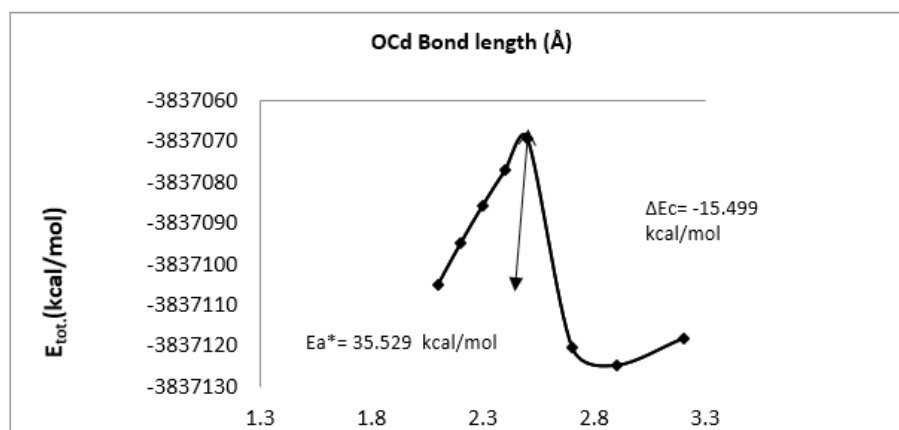


Figure 7. Potential energy curve for O-Cd energy bond rupture in  $\text{Al}_2\text{O}_3$  using ab initio U-DFT method.

#### 4- CONCLUSIONS

$\gamma\text{-Al}_2\text{O}_3$  nanoparticles was synthesized by electrochemical method and This is a simple and efficient method for preparing  $\gamma\text{-Al}_2\text{O}_3$  nanoparticles. The prepared materials had been characterized using X-Ray Diffraction Analysis (XRD) and Transmittance Electron microscope (TEM). Results show that the as-prepared sample had a size of  $\gamma\text{-Al}_2\text{O}_3$  nanoparticles ranged from 14 to 19 nanometers. The adsorption experiments revealed that the synthesized  $\gamma\text{-Al}_2\text{O}_3$  nanoparticles are effective in releasing  $\text{Cd}^{+2}$  from aqueous solutions. The adsorption process of cadmium was endothermic and reached equilibrium in 100 minutes. The equilibrium adsorption data undergo the Freundlich isotherm model better than the other models (Langmuir model). The  $\Delta G$  value was negative, which indicates that the adsorption spontaneous in nature. The results obtained from DFT study indicated that the Electrostatic surface workable signify the direct adsorption of molecule surface cadmium ion in accordance to more nucleophilic sites and Easily remove the ions from the  $\gamma\text{-Al}_2\text{O}_3$  nanoparticles molecule after adsorption. Present work expected that aluminum oxide nanoparticles, as well gamma  $\text{Al}_2\text{O}_3$  as a new type of adsorbents.

#### ACKNOWLEDGEMENT

The author Dhia H. Hussain and Shaimaa H. Jaber are grateful to the staff of the physical chemistry research laboratory of the College of Science of University of Mustansiriyah for their assistance during the laboratory work.

#### REFERENCES

1. Tang B., Ge J., Zhuo L., Wang G., Niu J., Shi Z. and Dong Y., A facile and controllable synthesis of  $\gamma$ -alumina nano-structure without a surfactant. *Eur. J. Inorg. Chem.*, **21**, 4366-4369(2005).
2. Zhou S., Antonietti M. and Niederberger M., Low temperature synthesis of  $\gamma$ -alumina nanocrystals from aluminium acetylacetonate in nonaqueous media. *Small*, **3**(5), 763-767(2007).
3. Reddy B.S.B., Das K. and Das S., A review on synthesis of in situ aluminium based composites by thermal, mechanical and mechanical thermal activation of chemical reactions. *J. Mater. Sci.*, **42**(22), 9366-9378(2007).
4. Lang Y., Wang Q., Xing J., Zhang B. and Liu H., Preparation of magnetic  $\gamma\text{-Al}_2\text{O}_3$  supported palladium catalyst for hydrogenation of nitrobenzene. *Process Syst. Eng.*, **54**(9), 2303-2309(2008).
5. Kobayashi Y., Ishizaki T. and Kurokawa Y., Preparation of alumina films by sol-gel method. *J. Mater. Sci.*, **40**(2) 263-283(2005).
6. Bahlawane N. and Watanabe T. New Sol-Gel Route for the Preparation of Pure Alpha-Alumina at 950 Degrees C. *Journal of the American Ceramic Society*, **83**(9), 2324-2326(2000).

7. Abbas. W. S., Rosenani A. H., Mustafa M. K., Frederick P. M. and Ponnadurai R., Novel triazine-functionalized tetra imidazolium hexafluorophosphate salt: Synthesis, crystal structure and DFT study. *Journal of Molecular Structure*, **1198**, 126902(2019).
8. Rana A. A., Ivan H. R. T., Majid H. A., Shaimaa A.N. and Mustafa M. K., Expired Etoricoxib as a corrosion inhibitor for steel in acidic solution. *Journal of Molecular Liquids*, **279**, 594–602(2019).
9. Ahmad M. A., Rahdar A., Sadeghfar F., Bagheri S. and Hajinezhad M. R., *Nanomedicine Research J.*, **1**(1), 39-46(2016).
10. Ammar N. , Youssef A.F.A. , Kenawy S. H., Hamzawy E.M.A. and El-Khateeb M.A., Wollastonite Ceramic/CuO Nano-Composite for Cadmium Ions Removal from Waste Water. *Egypt. J. Chem.* **60**(5), 817 - 823 (2017)
11. Weber Jr.W.J., Morris J.C. and Sanit J., Kinetics of Adsorption on Carbon from Solution. *Journal of the Sanitary Engineering Division, American Society of Civil Engineers* **89**, 31-38(1963).
12. Frisch, M.J., Trucks, G.W., Schlegel, H.B., Scuseria, G.E., Robb, M.A., Cheeseman, J.R., Montgomery, J.A., Jr., Vreven, T., Kudin, K.N., Burant, J.C., Millam, J.M., Iyengar, S.S., Tomasi, J., Barone, V., Mennucci, B., Cossi, M., Scalmani, G., Rega, N., Petersson, G.A., Nakatsuji, H., Hada, M., Ehara, M., Toyota, K., Fukuda, R., Hasegawa, J., Ishida, M., Nakajima, T., Honda, Y., Kitao, O., Nakai, H., Klene, M., Li, X., Knox, J.E., Hratchian, H.P. Cross, J.B. Bakken, V. Adamo, C. Jaramillo, J., Gomperts, R., Stratmann, R.E., Yazyev, O., Austin, A.J., Cammi, R., Pomelli, C., Ochterski, J.W., Ayala, P.Y., Morokuma, K., Voth, G.A., Salvador, P., Dannenberg, J.J., Zakrzewski, V.G., Dapprich, S., Daniels, A.D., Strain, M.C., Farkas, O., Malick, D.K., Rabuck, A.D., Raghavachari, K., Foresman, J.B., Ortiz, J.V., Cui, Q., Baboul, A.G., Clifford, S., Cioslowski, J., Stefanov, B.B., Liu, G., Liashenko, A., Piskorz, P., Komaromi, I., Martin, R.L., Fox, D.J., Keith, T., Al-Laham, M.A., Peng, C.Y., Nanayakkara, A., Challacombe, M., Gill, P.M.W., Johnson, B., Chen, W., Wong, M.W., Gonzalez, C. and Pople, J.A., Gaussian 09, Revision E.01. Gaussian, Inc. Wallingford CT, (2009).
13. Becke, A.D., Density-functional thermochemistry. III. The role of exact exchange. *J. Chem. Phys.*, **98**, 5648-5652(1993).
14. Ee, C., Yang, W. and Parr, R.G., Development of the Colle-Salvetti correlation energy formula into a functional of the electron density. *Phys. Rev.*, B **41**, 785-789(1988).
15. Parr, R.G. and Yang, W., Density functional approach to the frontier-electron theory of chemical reactivity. *Chem. Phys.*, **106**, 4049–4050(1984).
16. Shanshal M., Muala M.M., C-C Bond Cleavage in Aromatic Molecules; Benzene, Toluene and Naphthalene. *Jordan J Chem*, **8**(2) 113 (2013).
17. Kubba R. M., Theoretical study of IR spectra; Reaction Energies of C-O Thermal Bond Rupture in Some Ampicillin Prodrugs, Nahrrain university journal of science chemistry, **15**(1) 1-11 (2012).
18. Kubba R.M and Al. Mouamin T. M., Quantum Mechanical Calculations of IR Spectra; Reaction Energies of C-O (R-O) Thermal Bond Rupture for Cefuroxime Prodrugs, Anbar journal of pure science, **6**(3) 90-101 (2012)..
19. Kubba R. M., Quantum Mechanical Calculations of R-O Thermal Bond Rupture Energies in Some Ampicillin Prodrugs, Iraqi journal of Science **54**, 739-752 (2013).
20. Nematov D. D., Burhonzoda A. S., Khusenov M. A., Kholmurodov K. T. and Ibrahim M. A.A., The Quantum-Chemistry Calculations of Electronic Structure of Boron Nitride Nanocrystals with Density Functional Theory Realization. *Egypt. J. Chem. The First International Conference on Molecular Modeling and Spectroscopy*, pp. 21- 27 (2019)